

Revealing Neutrino Mass Ordering at CEPC and FCC-ee

Wei Liu,^{1,*} Supriya Senapati,^{1,†} and Jin Sun^{2,‡}

¹*Department of Applied Physics and MIIT Key Laboratory of Semiconductor Microstructure and Quantum Sensing, Nanjing University of Science and Technology, Nanjing 210094, China*

²*Particle Theory and Cosmology Group, Center for Theoretical Physics of the Universe, Institute for Basic Science (IBS), Daejeon 34126, Korea*

The neutrino masses ordering remains one of the most important open questions in neutrino physics. While upcoming oscillation experiments aim to resolve this problem at low energies, complementary approaches are highly desirable. In this Letter, we show that the neutrino mass ordering can be probed at high-energy colliders through the lepton-flavor structure of heavy neutral lepton (HNL) interactions. In the minimal Type-I seesaw scenario with two nearly degenerate HNLs, the heavy-light neutrino mixings are strongly correlated with the light-neutrino mass spectrum, leading to distinct flavor patterns for the normal and inverted hierarchies. We demonstrate that future Z factories, such as CEPC and FCC-ee, can probe the neutrino mass ordering for total HNL mixings as small as $U_{\text{tot}}^2 \gtrsim 4 \times 10^{-9}$, and discriminate between the two hierarchies for $U_{\text{tot}}^2 \gtrsim 10^{-6}$. Our results establish collider searches for HNLs as a powerful and complementary probe of the neutrino mass ordering.

Introduction Neutrino oscillation experiments [1] allow two possible neutrino mass orderings: the **normal hierarchy (NH)**, $m_3 > m_2 > m_1$, and the **inverted hierarchy (IH)**, $m_2 > m_1 > m_3$, with neutrino masses below the eV scale. Determining the true neutrino mass ordering is a central open question in particle physics, with profound implications for the origin of neutrino mass, neutrinoless double beta decay, and the matter-antimatter asymmetry of the Universe. While upcoming experiments such as JUNO [2], DUNE [3], and Hyper-Kamiokande [4] aim to resolve this question through precision measurements of neutrino oscillations at low energies, complementary probes from other frontiers are equally essential.

Heavy neutral leptons (HNLs), predicted in the Type-I seesaw mechanism [5–8], provide a complementary probe of neutrino mass generation at high-energy colliders. These heavy Majorana fermions mix weakly with the active neutrinos, with mixings parametrized by $|U_{\alpha N}|^2$ ($\alpha = e, \mu, \tau$), and N represents the mass eigenstates of the HNLs. However, existing collider searches mainly focused on single-flavor mixing scenarios, they are generally insensitive to the neutrino mass ordering [9–33]. In this Letter, we show that collider experiments can determine the mass ordering by exploiting the flavor structure of HNL interactions.

To reproduce neutrino oscillation data, at least two HNLs are required. In the minimal seesaw scenario with two nearly degenerate HNLs, the HNL flavor mixings are strongly correlated with the light-neutrino mass spectrum. In particular, the mixings inherit the flavor structure of the heaviest light-neutrino states, leading to a suppressed electron mixing in the NH, $|U_{eN}^2| \ll |U_{\mu N}^2| \sim |U_{\tau N}^2|$, whereas comparable mixings among all flavors are expected in the IH, $|U_{eN}^2| \sim |U_{\mu N}^2| \sim |U_{\tau N}^2|$ [34, 35]. Consequently, the comparison of lepton-flavor final states in HNL decays provides an indirect handle on the neutrino mass ordering.

Future Z factories, such as CEPC and FCC-ee, offer an ideal environment to test this idea due to the large statistics of HNLs production. We quantify the sensitivity to the mass ordering in the seesaw parameter space (m_N, U_{tot}^2) and demonstrate that colliders can provide a complementary determination of the mass ordering.

Lepton Flavor Mixing of the HNL In the minimal Type-I seesaw scenario with two nearly degenerate HNLs N_I ($I = 1, 2$), the heavy-light mixing parameters $\Theta_{\alpha I}$ not only govern the production and decay of HNLs at colliders, but also encode the flavor structure imprinted by the light-neutrino mass spectrum. As a result, the relative strengths of the HNL couplings to the electron, muon, and tau flavors depend sensitively on the neutrino mass ordering. In particular, the NH predicts a suppressed electron mixing due to the vanishing lightest neutrino

* wei.liu@njust.edu.cn

† ssenapati@njust.edu.cn

‡ sunjin0810@ibs.re.kr (Contact author)

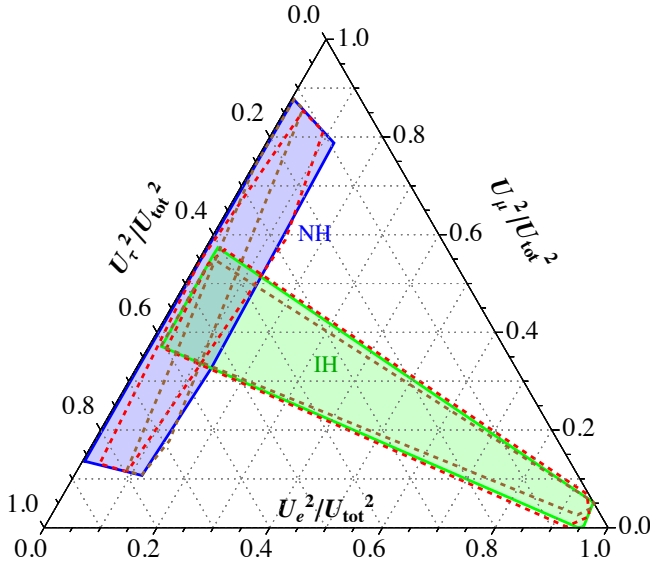


FIG. 1. Ternary plot showing the distribution of flavor-mixing ratios $U_\alpha^2/U_{\text{tot}}^2$, $\alpha = e, \mu, \tau$ for NH (blue) and IH (green). They are obtained by NuFIT 6.0 [37, 38] and JUNO’s latest result [39]. The dashed red (brown) curve shows the region under the best-fit CP phase from T2K (NO ν A), assuming a future uncertainty of 8° (7°) from DUNE+ μ THEIA [40].

mass, whereas the IH leads to a more democratic flavor pattern. This makes the lepton-flavor composition of HNL interactions a sensitive probe of the mass ordering.

The experimentally measurable quantities $U_{\alpha N}^2$ arise from the cumulative effects of both N_1 and N_2 , expressed as [36]

$$\begin{aligned}
 U_{\alpha N}^2 &= \sum_I |\Theta_{\alpha I}|^2 = \frac{1}{2m_N} (|c_\alpha^+|^2 x_\omega^2 + |c_\alpha^-|^2 x_\omega^{-2}), \\
 \text{NH : } c_\alpha^\pm &= iV_{\alpha 2}^{\text{PMNS}} \sqrt{m_2} \pm V_{\alpha 3}^{\text{PMNS}} \sqrt{m_3}, \\
 U_{\text{tot}}^2 &= \sum_{\alpha, I} |\Theta_{\alpha I}|^2 = \frac{(m_2 + m_3)}{2m_N} (x_\omega^2 + x_\omega^{-2}), \\
 \text{IH : } c_\alpha^\pm &= iV_{\alpha 1}^{\text{PMNS}} \sqrt{m_1} \pm V_{\alpha 2}^{\text{PMNS}} \sqrt{m_2}, \\
 U_{\text{tot}}^2 &= \sum_{\alpha, I} |\Theta_{\alpha I}|^2 = \frac{(m_1 + m_2)}{2m_N} (x_\omega^2 + x_\omega^{-2}). \quad (1)
 \end{aligned}$$

Here $U_{\alpha N}^2$ and U_{tot}^2 quantify the HNL mixing to a particular flavor and three flavors in total, respectively. And the rest of quantities are defined in the Appendix A. Eq. (1) shows explicitly that, in the minimal seesaw with two HNLs, the flavor composition of the heavy-light mixing is not arbitrary but is fully determined by the light-neutrino mass spectrum and the PMNS mixing matrix. Consequently, the HNL flavor ratios provide a direct imprint of the mass ordering.

Mass Ordering	$U_{eN}^2/U_{\text{tot}}^2$	$U_{\mu N}^2/U_{\text{tot}}^2$	$U_{\tau N}^2/U_{\text{tot}}^2$
NH	$(3.1 \times 10^{-3}, 0.14)$	$(0.11, 0.88)$	$(0.09, 0.86)$
IH	$(0.021, 0.96)$	$(0, 0.57)$	$(0, 0.61)$

TABLE I. The range of $U_{\alpha N}^2/U_{\text{tot}}^2$ for NH/IH mass orderings.

Following Eq. (1), we scan the neutrino oscillation parameters within their 3σ allowed ranges from NuFIT [37, 38] and JUNO’s latest result [39] to obtain the ternary distributions shown in Fig. 1. In the NH case, the absence of the ν_1 contribution, together with $|V_{e1}^{\text{PMNS}}| \gg |V_{e2,3}^{\text{PMNS}}|$, leads to a significantly suppressed electron mixing of the HNL. As a result, the allowed range of $U_{eN}^2/U_{\text{tot}}^2$ is confined to $(3.1 \times 10^{-3}, 0.14)$, as summarized in Table I.

Improved precision in neutrino oscillation measurements can further reduce the allowed parameter space. Although JUNO’s first results already demonstrate this potential [39], sizable uncertainties remain. Among the oscillation parameters, the Dirac CP phase δ_D is currently the least constrained and exhibits a notable tension between T2K [41] and NO ν A [42], with best-fit values of $\delta_D \simeq -\pi/2$ (T2K) and $\delta_D \simeq 148^\circ$ (NO ν A)¹. To illustrate its impact, Fig. 1 shows the predicted NH regions corresponding to the best-fit δ_D values from T2K (red dashed) and NO ν A (brown dashed), assuming future uncertainties of 8° and 7° , respectively, achievable with DUNE and μ THEIA [40]. In contrast, the IH region remains largely unchanged. This demonstrates that future precision measurements of δ_D will significantly sharpen the HNL flavor predictions.

Sensitivity on neutrino mass ordering The distinct flavor structures of HNL mixings associated with NH and IH provide a novel way to probe the neutrino mass ordering through the lepton-flavor composition of HNL decays at colliders, as discussed below.

To achieve large HNL statistics, we focus on future high-luminosity lepton colliders, in particular the Circular Electron–Positron Collider (CEPC) [44] and the Future Circular Collider in the electron–positron mode (FCC-ee) [45]. Our analysis targets the Z pole, corre-

¹ Recent combined analyses have partially reduced this tension [43].

sponding to a center-of-mass energy of $\sqrt{s} = 91.2$ GeV, with an integrated luminosity of $\mathcal{L} \simeq 200 \text{ ab}^{-1}$.

The signal process consists of single-HNL production in association with a neutrino or antineutrino, followed by its decay predominantly into a charged lepton and a pair of jets,

$$e^+ e^- \rightarrow N \nu (\bar{\nu}), \quad N \rightarrow \ell_\alpha jj, \quad (2)$$

where $\ell_\alpha = e, \mu$ denotes the charged lepton in the final state. Final states involving τ leptons are neglected due to the limited reconstruction efficiency and larger associated uncertainties. To ensure precise lepton-flavor identification and sufficient event statistics, we focus on prompt HNL decays, requiring the decay length in the laboratory frame to satisfy $L_N \lesssim 1$ mm. Alternative facilities, such as a muon collider [46–48] and μ TRISTAN [49], can also probe HNL production. However, for the processes considered here, the corresponding production cross sections are significantly suppressed compared to those at CEPC and FCC-ee. We therefore restrict our collider analysis to electron–positron machines.

Using MG5_AMC@NLO [50], event samples are generated with selection criteria requiring leptons and jets to lie within a pseudorapidity range of $|\eta| < 2.5$ and to satisfy $p_T(j/\ell) > 10$ GeV. The expected number of signal events in each lepton flavor channel is given by

$$N_{S,\alpha} = \sigma(Z) \times \text{Br}(Z \rightarrow N \nu (\bar{\nu})) \times \text{Br}(N \rightarrow \ell_\alpha jj) \times \mathcal{L} \times \epsilon, \quad (3)$$

where $\text{Br}(Z \rightarrow N \nu (\bar{\nu})) \propto U_{\text{tot}}^2$ and $\text{Br}(N \rightarrow \ell_\alpha jj) \propto U_{\alpha N}^2/U_{\text{tot}}^2$. The overall efficiency is factorized as $\epsilon \simeq \epsilon_{\text{prompt}} \times \epsilon_{\text{recon}}$. The prompt-decay efficiency, $\epsilon_{\text{prompt}} \simeq 1 - e^{-l_{\text{dec}}/L_N}$, accounts for HNL decays occurring within the primary vertex resolution $l_{\text{dec}} \simeq 1$ mm, where the decay length L_N is given in Eq. (A7). For electrons and muons, both the CEPC and FCC-ee detectors are designed to achieve near-perfect reconstruction and identification performance. Full detector simulations indicate reconstruction efficiencies exceeding 99% for isolated leptons over a wide angular acceptance [51, 52].

Hence, for short-lived HNLs, the number of signal events can be well approximated as

$$N_{S,\alpha} \simeq \mathcal{O}(10^{11}) \times U_{\text{tot}}^2 \times R_\alpha \equiv N_0 \times R_\alpha, \quad (4)$$

where $R_\alpha \equiv U_{\alpha N}^2/U_{\text{tot}}^2$ encodes the flavor composition of the active–sterile mixing, and $N_0 \sim \mathcal{O}(10^{11}) \times U_{\text{tot}}^2$

denotes the total number of signal events, which is independent of flavor.

The dominant Standard Model background arises from irreducible diboson processes. Applying the same selection criteria, we find

$$N_{B,\alpha} \simeq 1.4 \times 10^5, \quad (5)$$

per flavor for $\alpha = e, \mu$.

To probe the neutrino mass ordering, we analyze the signal and background distributions in the two-flavor plane (R_e, R_μ) , which directly maps onto the ternary regions shown in Fig. 1. For a fixed value of U_{tot}^2 , we define the detection significance as

$$\chi_{\text{NH/IH}}^2 = \sum_{\alpha=e,\mu} \frac{\left[N_0 \left(R_\alpha^{\text{obs}} - R_\alpha^{\text{NH/IH}} \right) \right]^2}{N_0 R_\alpha^{\text{NH/IH}} + N_{B,\alpha}}, \quad (6)$$

where R_α^{obs} denotes the observed flavor fraction, and $R_\alpha^{\text{NH/IH}}$ is the theoretical prediction under the normal or inverted mass ordering. Requiring $\min(\chi_{\text{NH/IH}}^2) > 4$, we can exclude the NH or IH hypothesis at approximately the 2σ level.

In Fig. 2, we present the sensitivity to the neutrino mass ordering in the (R_e, R_μ) plane for $U_{\text{tot}}^2 \simeq 10^{-5}$ (a), 10^{-7} (b), 10^{-8} (c), and 4×10^{-9} (d), respectively, assuming $m_N \simeq 50$ GeV. $\chi_{\text{NH/IH}}^2$ is evaluated by taking R_α^{obs} to coincide with the coordinates in the (R_e, R_μ) plane, while $R_\alpha^{\text{NH/IH}}$ corresponds to the regions predicted for NH (blue dashed) and IH (green dashed) hypotheses.

Following Table II, the figure distinguishes four regions according to their capability to test the NH and IH hypotheses. As U_{tot}^2 increases in Fig. 2, the resulting growth in the $\chi_{\text{NH/IH}}^2$ leads to three correlated effects: (i) an expansion of the excluded region, (ii) a contraction of the ambiguous region where the NH and IH cannot be distinguished, and (iii) a convergence of the NH- or IH-favored regions toward their respective theoretically predicted parameter spaces. Taken together, these effects substantially enhance the discrimination power between the two neutrino mass orderings.

To quantify the overall discrimination power, we define the fraction of parameter space (in \log_{10} scale) for which the neutrino mass ordering can be unambiguously identified,

$$K = 1 - \frac{S_{\text{NH} \cap \text{IH}}}{S_{\text{tot}}}, \quad (7)$$

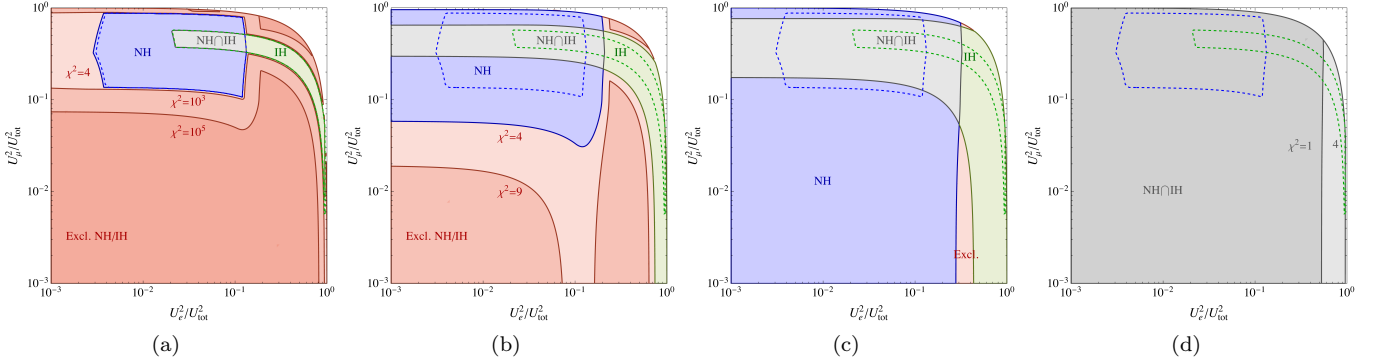


FIG. 2. Sensitivity of the neutrino mass orderings in the plane of $(U_{eN}^2/U_{\text{tot}}^2, U_{\mu N}^2/U_{\text{tot}}^2)$, at $\sqrt{s} = 91.2$ GeV CEPC/FCC-ee with $\mathcal{L} \approx 200 \text{ ab}^{-1}$, for $U_{\text{tot}}^2 \approx 10^{-5}$ (a), 10^{-7} (b), 10^{-8} (c), and 4×10^{-9} (d), respectively, when $m_N \sim 50$ GeV.

Region	Color	$\min(\chi_{NH}^2)$	$\min(\chi_{IH}^2)$
NH Favor	Blue	< 4	> 4
IH Favor	Green	> 4	< 4
NH ∩ IH Favor	Gray	< 4	< 4
Excluded	Red	> 4	> 4

TABLE II. The NH, IH, NH/IH Favor and Excluded Regions in Fig. 2 and their range of $\min(\chi_{NH}^2, \chi_{IH}^2)$.

where $S_{\text{NH} \cap \text{IH}}$ denotes the area of the region in which both the NH and IH hypotheses are allowed, and S_{tot} is the total area spanned by the theoretically predicted NH and IH parameter spaces. The quantity K therefore provides a global measure of the fraction of the allowed seesaw parameter space that permits an unambiguous determination of the neutrino mass ordering, rather than a confidence level associated with a single parameter point.

Owing to the intrinsic overlap between the predicted NH and IH regions, we find $K \lesssim 0.90$ even in the limit of large event statistics. When $N_0 \lesssim 2\sqrt{\sum_{\alpha=e,\mu} N_{B,\alpha}}$, the excluded region disappears, while the overlap region ($\text{NH} \cap \text{IH}$) covers almost the entire parameter space, driving $K \simeq 0$.

In Fig. 3 we show contours of the fraction K in the (m_N, U_{tot}^2) plane, together with existing bounds and future sensitivities. Cosmological observations from Planck constrain the sum of light neutrino masses, $\sum_i m_{\nu_i} \simeq U_{\text{tot}}^2 m_N \lesssim 0.12$ eV, via the seesaw relation [55]. Bounds from charged lepton radiative decays, $\text{Br}(\ell_\alpha \rightarrow \ell_\beta \gamma) \propto U_\alpha^2 U_\beta^2$, are shown by the black curves for NH (solid) and IH (dashed), with details given in the Appendix A. The CEPC/FCC-ee sensitivity is kinematically suppressed as $m_N \lesssim 70$ GeV.

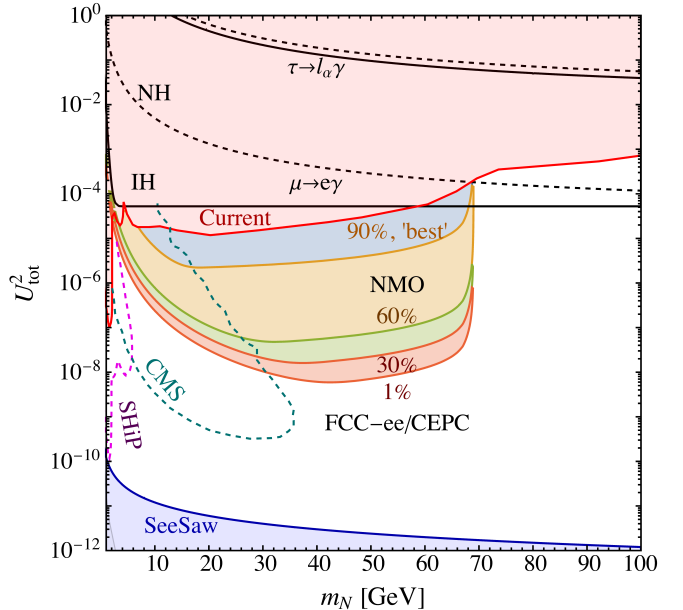


FIG. 3. Fraction of the parameter space (in \log_{10} scale) that allows unambiguous identification of the neutrino mass ordering (NMO) via $e^+e^- \rightarrow N\nu(\bar{\nu})$, followed by $N \rightarrow \ell_\alpha jj$, at $\sqrt{s} = 91.2$ GeV for CEPC/FCC-ee with $\mathcal{L} \simeq 200 \text{ ab}^{-1}$. Regions with $K > 1\%$ (30%, 60%, 90%) and $K < 30\%$ (60%, 90%) are shaded in red (green, orange, and cyan), respectively. The red area labeled “Current” is excluded by existing constraints [13], while dashed contours labeled “SHiP” and “CMS” indicate future sensitivities [53, 54]. The black line denotes the bound from $\ell_\alpha \rightarrow \ell_\beta \gamma$, for NH (dashed) and IH (solid). The “Seesaw” region reflects the cosmological bound $\sum_i m_{\nu_i} \simeq U_{\text{tot}}^2 m_N \lesssim 0.12$ eV with $i = 1, 2, 3$ from Planck data [55].

Although CEPC/FCC-ee cannot directly probe the seesaw limit, they exhibit strong discriminating power for the neutrino mass ordering: $K \simeq 1\%$ for $U_{\text{tot}}^2 \simeq 4 \times 10^{-9}$, rising to $K \simeq 30\%$ (60%) for $U_{\text{tot}}^2 \simeq 10^{-8}$ (10^{-7}). Near-

maximal discrimination, $K \simeq 90\%$, approaching the limit set by current oscillation data, remains attainable for $U_{\text{tot}}^2 \gtrsim 10^{-6}$, about one order of magnitude below existing experimental bounds.

Conclusion In this Letter, we have demonstrated that the neutrino mass ordering can be probed at high-energy colliders through the flavor structure of HNL interactions. Within the minimal Type-I seesaw framework with two nearly degenerate HNLs, the heavy–light neutrino mixings are strongly correlated with the light-neutrino mass spectrum, yielding characteristic and distinguishable flavor patterns for the NH and IH.

Focusing on future Z factories such as CEPC and FCC-ee, we show that the lepton-flavor composition of prompt HNL decays provides a robust handle on the neutrino mass ordering. For total mixings as small as $U_{\text{tot}}^2 \simeq 4 \times 10^{-9}$, collider measurements can already probe the mass-ordering-sensitive parameter space. For larger mixings, $U_{\text{tot}}^2 \gtrsim 10^{-6}$, a near-maximal discrimination power can be achieved, approaching the limit imposed by current neutrino oscillation data.

Our results highlight a unique synergy between collider experiments and neutrino oscillation measurements. While experiments like JUNO probe the infrared properties of the neutrino mass spectrum, CEPC and FCC-ee directly access its ultraviolet origin through the HNL flavor structure. A consistent determination of the mass ordering across these complementary frontiers would provide compelling evidence for the minimal seesaw mechanism with two HNLs, whereas any tension would signal new dynamics beyond this minimal framework.

ACKNOWLEDGMENTS

We thank F. F. Deppisch and Chayan Majumdar for useful discussions. W. L. is supported by National Natural Science foundation of China (Grant No. 12205153). J. S. was supported by IBS under the project code, IBS-R018-D1. The authors gratefully acknowledge the valuable discussions and insights provided by the members of the China Collaboration of Precision Testing and New Physics (CPTNP).

Appendix A: Type-I seesaw framework

We consider a minimal Type-I seesaw with two heavy neutral leptons (HNLs) ν_{RI} ($I = 1, 2$), sufficient to reproduce neutrino oscillation data. The relevant Lagrangian is

$$\mathcal{L} = i\bar{\nu}_{RI}\not{\partial}\nu_{RI} - Y_{\alpha I}(\bar{L}_{\alpha} \cdot \tilde{H})\nu_{RI} - \frac{1}{2}M_I\bar{\nu}_{RI}^c\nu_{RI}, \quad (\text{A1})$$

where $\alpha = e, \mu, \tau$ and M_I is taken diagonal. After electroweak symmetry breaking, $m_D = Yv/\sqrt{2}$, and the neutrino mass matrix reads

$$\mathcal{L}_m = -\frac{1}{2}(\bar{\nu}_L^c\bar{\nu}_R)\begin{pmatrix} 0 & m_D^T \\ m_D & m_R \end{pmatrix}\begin{pmatrix} \nu_L^c \\ \nu_R \end{pmatrix}. \quad (\text{A2})$$

In the seesaw limit $m_D \ll m_R$, the light neutrino mass matrix is $m_{\nu} \simeq -m_D^T m_R^{-1} m_D$. The flavor eigenstates are related to mass eigenstates by

$$\nu_{L\alpha} = V_{\alpha i}^{\text{PMNS}}\nu_i + \Theta_{\alpha I}N_I^c, \quad \Theta_{\alpha I} \simeq \frac{vY_{\alpha I}}{M_I}. \quad (\text{A3})$$

We employ the Casas–Ibarra parametrization [56],

$$m_D = iV^{\text{PMNS}}\sqrt{m_{\nu}^{\text{diag}}}R\sqrt{m_R^{\text{diag}}}, \quad (\text{A4})$$

with $m_R^{\text{diag}} = \text{diag}(M_1, M_2)$. For normal (inverted) ordering, $m_1 = 0$ ($m_3 = 0$), and the complex orthogonal matrix R is

$$R^{\text{NH}} = \begin{pmatrix} 0 & 0 \\ \cos\omega & \sin\omega \\ -\sin\omega & \cos\omega \end{pmatrix}, \quad R^{\text{IH}} = \begin{pmatrix} \cos\omega & \sin\omega \\ -\sin\omega & \cos\omega \\ 0 & 0 \end{pmatrix}, \quad (\text{A5})$$

where ω is complex and we define $x_{\omega} \equiv e^{\text{Im}\omega}$. Majorana phases are included through the PMNS matrix.

The charged-current interaction in the mass basis is

$$-\mathcal{L}_{\text{CC}} = \frac{g}{\sqrt{2}}W_{\mu}^{+}\sum_{\ell}\left(\sum_{i=1}^3V_{\ell i}^{*}\bar{\nu}_i + \sum_{I=1}^2\Theta_{\ell I}^{*}\bar{N}_I^c\right)\gamma^{\mu}P_L\ell + \text{h.c.} \quad (\text{A6})$$

For $M_1 \simeq M_2$ and $\Theta_{\ell 1} = \pm i\Theta_{\ell 2}$, the two HNLs form a pseudo-Dirac fermion with an approximate $U(1)$ symmetry.

HNLs decay via off-shell W/Z bosons into leptonic and semileptonic final states. The decay length in the laboratory frame is approximately [57]

$$L_N \simeq \frac{1.6}{U_{\text{tot}}^2} \left(\frac{m_N}{\text{GeV}}\right)^{-6} \left(1 - \frac{m_N^2}{m_Z^2}\right) \text{cm}. \quad (\text{A7})$$

Existing constraints on active–sterile mixing are summarized in Ref. [13]. Mixing among different flavors induces radiative decays $\ell_i \rightarrow \ell_j \gamma$ at one loop [58, 59]. The strongest bound arises from MEG II, $\text{Br}(\mu \rightarrow e\gamma) < 1.5 \times 10^{-13}$ [60], with additional limits from $\tau \rightarrow \ell\gamma$ searches [61, 62]. Future displaced-vertex searches at CMS [54] and the SHiP beam-dump experiment [53, 63] provide complementary sensitivity, particularly in the long-lived HNL regime.

Appendix B: Background at Collider

The irreducible four-fermion Standard Model background for CEPC and FCC-ee operating at the Z pole, $e^+e^- \rightarrow \mu\nu jj$, is generated at leading order using MG5_AMC@NLO. The simulation includes contributions from both associated production via on-shell and off-shell W bosons, as well as from Z/γ^* production followed by radiation of an off-shell W from one of the Z decay legs. Other Standard Model backgrounds, including ZZ , WZ , $Z\nu\bar{\nu}$, top-quark, and multiboson processes, are neglected, as they either produce additional visible objects or require misidentification to mimic the exclusive one lepton and two jet final state. The resulting leading-order cross section for the background is found to be 0.72 fb per flavor.

[1] Particle Data Group Collaboration, S. Navas et al., *Review of particle physics*, *Phys. Rev. D* **110** (2024), no. 3 030001.

[2] JUNO Collaboration, Z. Djurcic et al., *JUNO Conceptual Design Report*, [arXiv:1508.07166](https://arxiv.org/abs/1508.07166).

[3] DUNE Collaboration, B. Abi et al., *Deep Underground Neutrino Experiment (DUNE), Far Detector Technical Design Report, Volume I Introduction to DUNE*, *JINST* **15** (2020), no. 08 T08008, [arXiv:2002.02967](https://arxiv.org/abs/2002.02967).

[4] Hyper-Kamiokande Collaboration, K. Abe et al., *Hyper-Kamiokande Design Report*, [arXiv:1805.04163](https://arxiv.org/abs/1805.04163).

[5] P. Minkowski, $\mu \rightarrow e\gamma$ at a Rate of One Out of 10^9 Muon Decays?, *Phys. Lett. B* **67** (1977) 421–428.

[6] T. Yanagida, Horizontal Symmetry and Masses of Neutrinos, *Prog. Theor. Phys.* **64** (1980) 1103.

[7] M. Gell-Mann, P. Ramond, and R. Slansky, Complex Spinors and Unified Theories, *Conf. Proc. C* **790927** (1979) 315–321, [arXiv:1306.4669](https://arxiv.org/abs/1306.4669).

[8] R. N. Mohapatra and G. Senjanovic, Neutrino Mass and Spontaneous Parity Nonconservation, *Phys. Rev. Lett.* **44** (1980) 912.

[9] K. Kaneta, Z. Kang, and H.-S. Lee, Right-handed neutrino dark matter under the $B - L$ gauge interaction, *JHEP* **02** (2017) 031, [arXiv:1606.09317](https://arxiv.org/abs/1606.09317).

[10] K. Bondarenko, A. Boyarsky, D. Gorbunov, and O. Ruchayskiy, Phenomenology of GeV-scale Heavy Neutral Leptons, *JHEP* **11** (2018) 032, [arXiv:1805.08567](https://arxiv.org/abs/1805.08567).

[11] D. A. Bryman and R. Shrock, Constraints on Sterile Neutrinos in the MeV to GeV Mass Range, *Phys. Rev. D* **100** (2019) 073011, [arXiv:1909.11198](https://arxiv.org/abs/1909.11198).

[12] S. Balaji, M. Ramirez-Quezada, and Y.-L. Zhou, CP violation and circular polarisation in neutrino radiative decay, *JHEP* **04** (2020) 178, [arXiv:1910.08558](https://arxiv.org/abs/1910.08558).

[13] P. D. Bolton, F. F. Deppisch, and P. S. Bhupal Dev, Neutrinoless double beta decay versus other probes of heavy sterile neutrinos, *JHEP* **03** (2020) 170, [arXiv:1912.03058](https://arxiv.org/abs/1912.03058).

[14] W. Liu, K.-P. Xie, and Z. Yi, Testing leptogenesis at the LHC and future muon colliders: A Z' scenario, *Phys. Rev. D* **105** (2022), no. 9 095034, [arXiv:2109.15087](https://arxiv.org/abs/2109.15087).

[15] A. M. Abdullahi et al., The present and future status of heavy neutral leptons, *J. Phys. G* **50** (2023), no. 2 020501, [arXiv:2203.08039](https://arxiv.org/abs/2203.08039).

[16] Y. Zhang and W. Liu, Probing active-sterile neutrino transition magnetic moments at LEP and CEPC, *Phys. Rev. D* **107** (2023), no. 9 095031, [arXiv:2301.06050](https://arxiv.org/abs/2301.06050).

[17] D. Barducci, W. Liu, A. Titov, Z. S. Wang, and Y. Zhang, Probing the dipole portal to heavy neutral leptons via meson decays at the high-luminosity LHC, *Phys. Rev. D* **108** (2023), no. 11 115009, [arXiv:2308.16608](https://arxiv.org/abs/2308.16608).

[18] W. Liu, F. F. Deppisch, and Z. Chen, Testing leptogenesis and seesaw in the $B-L$ model using long-lived particle searches, *Phys. Rev. D* **110** (2024), no. 3 035017, [arXiv:2312.11165](https://arxiv.org/abs/2312.11165).

[19] W. Liu, S. Kulkarni, and F. F. Deppisch, Heavy neutrinos at the FCC-hh in the $U(1)B-L$ model, *Phys. Rev. D* **105** (2022), no. 9 095043, [arXiv:2202.07310](https://arxiv.org/abs/2202.07310).

[20] C. Han, T. Li, and C.-Y. Yao, Searching for heavy neutrino in terms of tau lepton at future hadron collider, *Phys. Rev. D* **104** (2021), no. 1 015036, [arXiv:2103.03548](https://arxiv.org/abs/2103.03548).

[21] A. Das and N. Okada, Bounds on heavy Majorana neutrinos in type-I seesaw and implications for collider searches, *Phys. Lett. B* **774** (2017) 32–40, [arXiv:1702.04668](https://arxiv.org/abs/1702.04668).

[22] A. Maiezza, M. Nemevšek, and F. Nesti, Lepton Number Violation in Higgs Decay at LHC, *Phys. Rev. Lett.* **115** (2015) 081802, [arXiv:1503.06834](https://arxiv.org/abs/1503.06834).

[23] F. F. Deppisch, W. Liu, and M. Mitra, Long-lived Heavy Neutrinos from Higgs Decays, *JHEP* **08** (2018) 181, [arXiv:1804.04075](https://arxiv.org/abs/1804.04075).

[24] J. D. Mason, *Time-Delayed Electrons from Higgs Decays to Right-Handed Neutrinos*, *JHEP* **07** (2019) 089, [[arXiv:1905.07772](#)].

[25] E. Accomando, L. Delle Rose, S. Moretti, E. Olaiya, and C. H. Shepherd-Themistocleous, *Novel SM-like Higgs decay into displaced heavy neutrino pairs in $U(1)$ models*, *JHEP* **04** (2017) 081, [[arXiv:1612.05977](#)].

[26] A. M. Gago, P. Hernández, J. Jones-Pérez, M. Losada, and A. Moreno Briceño, *Probing the Type I Seesaw Mechanism with Displaced Vertices at the LHC*, *Eur. Phys. J. C* **75** (2015), no. 10 470, [[arXiv:1505.05880](#)].

[27] J. Jones-Pérez, J. Masias, and J. D. Ruiz-Álvarez, *Search for Long-Lived Heavy Neutrinos at the LHC with a VBF Trigger*, *Eur. Phys. J. C* **80** (2020), no. 7 642, [[arXiv:1912.08206](#)].

[28] W. Liu, J. Li, J. Li, and H. Sun, *Testing the seesaw mechanisms via displaced right-handed neutrinos from a light scalar at the HL-LHC*, *Phys. Rev. D* **106** (2022), no. 1 015019, [[arXiv:2204.03819](#)].

[29] J. Li, W. Liu, and H. Sun, *Z' mediated right-handed neutrinos from meson decays at the FASER*, *Phys. Rev. D* **109** (2024), no. 3 035022, [[arXiv:2309.05020](#)].

[30] F. F. Deppisch, S. Kulkarni, and W. Liu, *Sterile Neutrinos at MAPP in the B-L Model*, 11, 2023, [[arXiv:2311.01719](#)].

[31] W. Liu, S. Kulkarni, and F. F. Deppisch, *Revealing the origin of neutrino masses through displaced shower searches in the CMS muon system*, *Phys. Rev. D* **111** (2025), no. 9 093003, [[arXiv:2407.20676](#)].

[32] Z. S. Wang, Y. Zhang, and W. Liu, *Searching for heavy neutral leptons coupled to axion-like particles at the LHC far detectors and SHiP*, *JHEP* **01** (2025) 070, [[arXiv:2409.18424](#)].

[33] Z. S. Wang, Y. Zhang, and W. Liu, *Long-lived sterile neutrinos from an axionlike particle at Belle II*, *Phys. Rev. D* **111** (2025), no. 3 035010, [[arXiv:2410.00491](#)].

[34] J.-L. Tastet, O. Ruchayskiy, and I. Timiryasov, *Reinterpreting the ATLAS bounds on heavy neutral leptons in a realistic neutrino oscillation model*, *JHEP* **12** (2021) 182, [[arXiv:2107.12980](#)].

[35] A. Abada, P. Escribano, X. Marcano, and G. Piazza, *Collider searches for heavy neutral leptons: beyond simplified scenarios*, *Eur. Phys. J. C* **82** (2022), no. 11 1030, [[arXiv:2208.13882](#)].

[36] S. Eijima, M. Shaposhnikov, and I. Timiryasov, *Parameter space of baryogenesis in the ν MSM*, *JHEP* **07** (2019) 077, [[arXiv:1808.10833](#)].

[37] I. Esteban, M. C. Gonzalez-Garcia, M. Maltoni, I. Martinez-Soler, J. P. Pinheiro, and T. Schwetz, *NuFit-6.0: updated global analysis of three-flavor neutrino oscillations*, *JHEP* **12** (2024) 216, [[arXiv:2410.05380](#)].

[38] I. Esteban, M. C. Gonzalez-Garcia, M. Maltoni, I. Martinez-Soler, J. P. Pinheiro, and T. Schwetz, *NuFit-6.0 (2024)*, <http://www.nu-fit.org>.

[39] **JUNO** Collaboration, A. Abusleme et al., *First measurement of reactor neutrino oscillations at JUNO*, [[arXiv:2511.14593](#)].

[40] S.-F. Ge, C.-F. Kong, and P. Pasquini, *Improving CP measurement with THEIA and muon decay at rest*, *Eur. Phys. J. C* **82** (2022), no. 6 572, [[arXiv:2202.05038](#)].

[41] **T2K** Collaboration, K. Abe et al., *Measurements of neutrino oscillation parameters from the T2K experiment using 3.6×10^{21} protons on target*, *Eur. Phys. J. C* **83** (2023), no. 9 782, [[arXiv:2303.03222](#)].

[42] **NOvA** Collaboration, M. A. Acero et al., *Improved measurement of neutrino oscillation parameters by the NOvA experiment*, *Phys. Rev. D* **106** (2022), no. 3 032004, [[arXiv:2108.08219](#)].

[43] **T2K, NOvA** Collaboration, S. Abubakar et al., *Joint neutrino oscillation analysis from the T2K and NOvA experiments*, *Nature* **646** (2025), no. 8086 818–824, [[arXiv:2510.19888](#)].

[44] **CEPC Study Group** Collaboration, C. S. Group, *CEPC Conceptual Design Report: Volume 1 - Accelerator*, [[arXiv:1809.00285](#)].

[45] **FCC** Collaboration, A. Abada et al., *FCC-ee: The Lepton Collider: Future Circular Collider Conceptual Design Report Volume 2*, *Eur. Phys. J. ST* **228** (2019), no. 2 261–623.

[46] T. H. Kwok, L. Li, T. Liu, and A. Rock, *Searching for heavy neutral leptons at a future muon collider*, *Phys. Rev. D* **110** (2024), no. 7 075009, [[arXiv:2301.05177](#)].

[47] P. Li, Z. Liu, and K.-F. Lyu, *Heavy neutral leptons at muon colliders*, *JHEP* **03** (2023) 231, [[arXiv:2301.07117](#)].

[48] K. Mkekala, J. Reuter, and A. F. Źarnecki, *Optimal search reach for heavy neutral leptons at a muon collider*, *Phys. Lett. B* **841** (2023) 137945, [[arXiv:2301.02602](#)].

[49] A. Das, J. Li, S. Mandal, T. Nomura, and R. Zhang, *Testing tree level TeV scale seesaw scenarios in μ TRISTAN*, *Phys. Rev. D* **112** (2025), no. 3 035008, [[arXiv:2410.21956](#)].

[50] J. Alwall, R. Frederix, S. Frixione, V. Hirschi, F. Maltoni, O. Mattelaer, H. S. Shao, T. Stelzer, P. Torrielli, and M. Zaro, *The automated computation of tree-level and next-to-leading order differential cross sections, and their matching to parton shower simulations*, *JHEP* **07** (2014) 079, [[arXiv:1405.0301](#)].

[51] **IDEA Study Group** Collaboration, M. Abbrescia et al., *The IDEA detector concept for FCC-ee*, [[arXiv:2502.21223](#)].

[52] X. Ai et al., *Flavor Physics at the CEPC: a General Perspective*, *Chin. Phys. C* **49** (2025), no. 10 103003, [[arXiv:2412.19743](#)].

[53] S. Alekhin et al., *A facility to Search for Hidden Particles at the CERN SPS: the SHiP physics case*, *Rept. Prog. Phys.* **79** (2016), no. 12 124201, [[arXiv:1504.04855](#)].

[54] M. Drewes and J. Hajer, *Heavy Neutrinos in displaced vertex searches at the LHC and HL-LHC*, *JHEP* **02** (2020) 070, [[arXiv:1903.06100](#)].

[55] **Planck** Collaboration, N. Aghanim et al., *Planck 2018 results. VI. Cosmological parameters*, *Astron. Astrophys.* **641** (2020) A6, [[arXiv:1807.06209](#)]. [Erratum: *Astron. Astrophys.* 652, C4 (2021)].

[56] J. A. Casas and A. Ibarra, *Oscillating neutrinos and $\mu \rightarrow e, \gamma$* , *Nucl. Phys. B* **618** (2001) 171–204, [[hep-ph/0103065](#)].

[57] M. Drewes, *Distinguishing Dirac and Majorana Heavy Neutrinos at Lepton Colliders*, *PoS ICHEP2022* (2022) 608, [[arXiv:2210.17110](#)].

[58] A. Ibarra, E. Molinaro, and S. T. Petcov, *Low Energy Signatures of the TeV Scale See-Saw Mechanism*, *Phys. Rev. D* **84** (2011) 013005, [[arXiv:1103.6217](#)].

[59] D. N. Dinh, A. Ibarra, E. Molinaro, and S. T. Petcov, *The $\mu - e$ Conversion in Nuclei, $\mu \rightarrow e\gamma$, $\mu \rightarrow 3e$ Decays and TeV Scale See-Saw Scenarios of Neutrino Mass Generation*, *JHEP* **08** (2012) 125, [[arXiv:1205.4671](https://arxiv.org/abs/1205.4671)]. [Erratum: *JHEP* **09**, 023 (2013)].

[60] **MEG II** Collaboration, K. Afanaciev et al., *New limit on the $\mu^+ \rightarrow e^+\gamma$ decay with the MEG II experiment*, *Eur. Phys. J. C* **85** (2025), no. 10 1177, [[arXiv:2504.15711](https://arxiv.org/abs/2504.15711)].

[61] **BaBar** Collaboration, B. Aubert et al., *Searches for Lepton Flavor Violation in the Decays $\tau^\pm \rightarrow e^\pm\gamma$ and $\tau^\pm \rightarrow \mu^\pm\gamma$* , *Phys. Rev. Lett.* **104** (2010) 021802, [[arXiv:0908.2381](https://arxiv.org/abs/0908.2381)].

[62] **Belle** Collaboration, A. Abdesselam et al., *Search for lepton-flavor-violating tau-lepton decays to $\ell\gamma$ at Belle*, *JHEP* **10** (2021) 19, [[arXiv:2103.12994](https://arxiv.org/abs/2103.12994)].

[63] **SHiP** Collaboration, C. Ahdida et al., *Sensitivity of the SHiP experiment to Heavy Neutral Leptons*, *JHEP* **04** (2019) 077, [[arXiv:1811.00930](https://arxiv.org/abs/1811.00930)].